The bioactive protein-ligand conformation of GluN2C-selective positive allosteric modulators bound to the NMDA receptor

Thomas M. Kaiser, Steven A. Kell, Hirofumi Kusumoto, Gil Shaulsky, Subhrajit Bhattacharya, Matthew P. Epplin, Katie L. Strong, Eric J. Miller, Bryan D. Cox, David S. Menaldino, Dennis C. Liotta, Stephen F. Traynelis and Pieter. B. Burger

Departments of Chemistry Emory University, Atlanta Georgia 30322 (T.M.K., S.A.K., M.P.E., K.L.S., E.J.M., B.D.C., D.S.M., D.C.L., P.B.B.); Department of Pharmacology Emory University School of Medicine, Atlanta, Georgia 30322 (K.H., G.S., S.B., S.F.T.)

Journal: Molecular Pharmacology

Data supplement:

Figure S1: 1D proton NMR spectrum of PYD-106.

Figure S2: 2D NOESY NMR spectrum of PYD-106 (400ms).

Figure S3: NMR experimental observations.

Figure S4: The alignment used for building in the linker region between ATD and ABD.

Supplemental Material S5: Attempt as separation of PYD enantiomers

Figure S6: The ROC curves and Enrichment plots of the *S*-enantiomer of 79 compounds representative of the PYD series docked to 9 homology models.

Figure S7: The ROC curves and Enrichment plots of the *R*-enantiomer of 79 compounds representative of the PYD series docked to 10 homology models.

Figure S8: Enrichment plot for PYD-series docked against the selected GluN2C homology model

Figure S9: Molecular overlay of the GluN1/GluN2C diheteromeric homology model and a diheteromeric GluN1/GluN2B Cryo-EM structure (PDBID: 5IOU)

Table S1: Shared sequence identity and similarity between NMDA subunits of the PYD binding pocket

PDB structures:

Ligand-receptor complex: A PDB structure of the ligand receptor complex of GluN2C and PYD-**106**

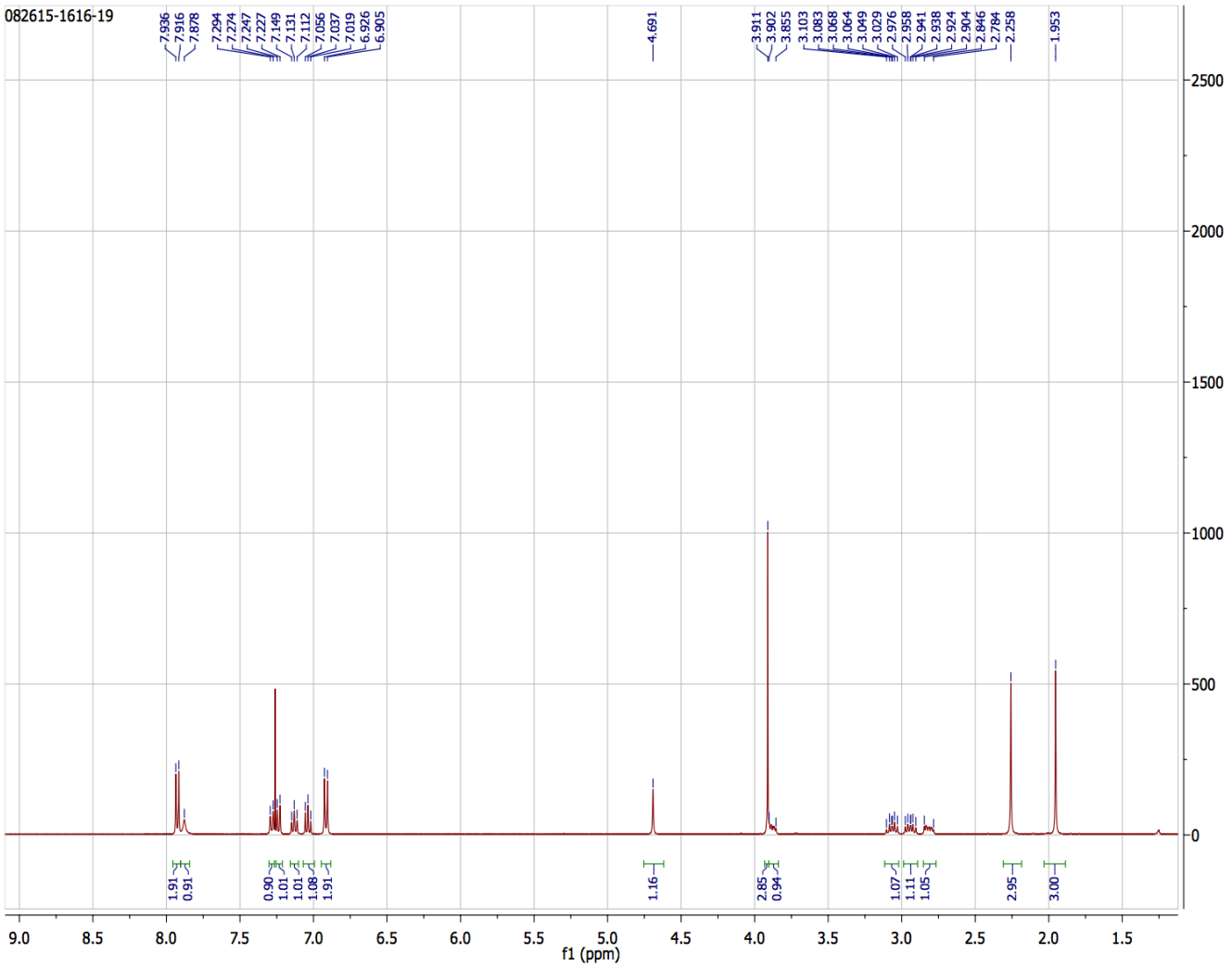

Figure S1: 1D proton NMR spectrum of PYD-106

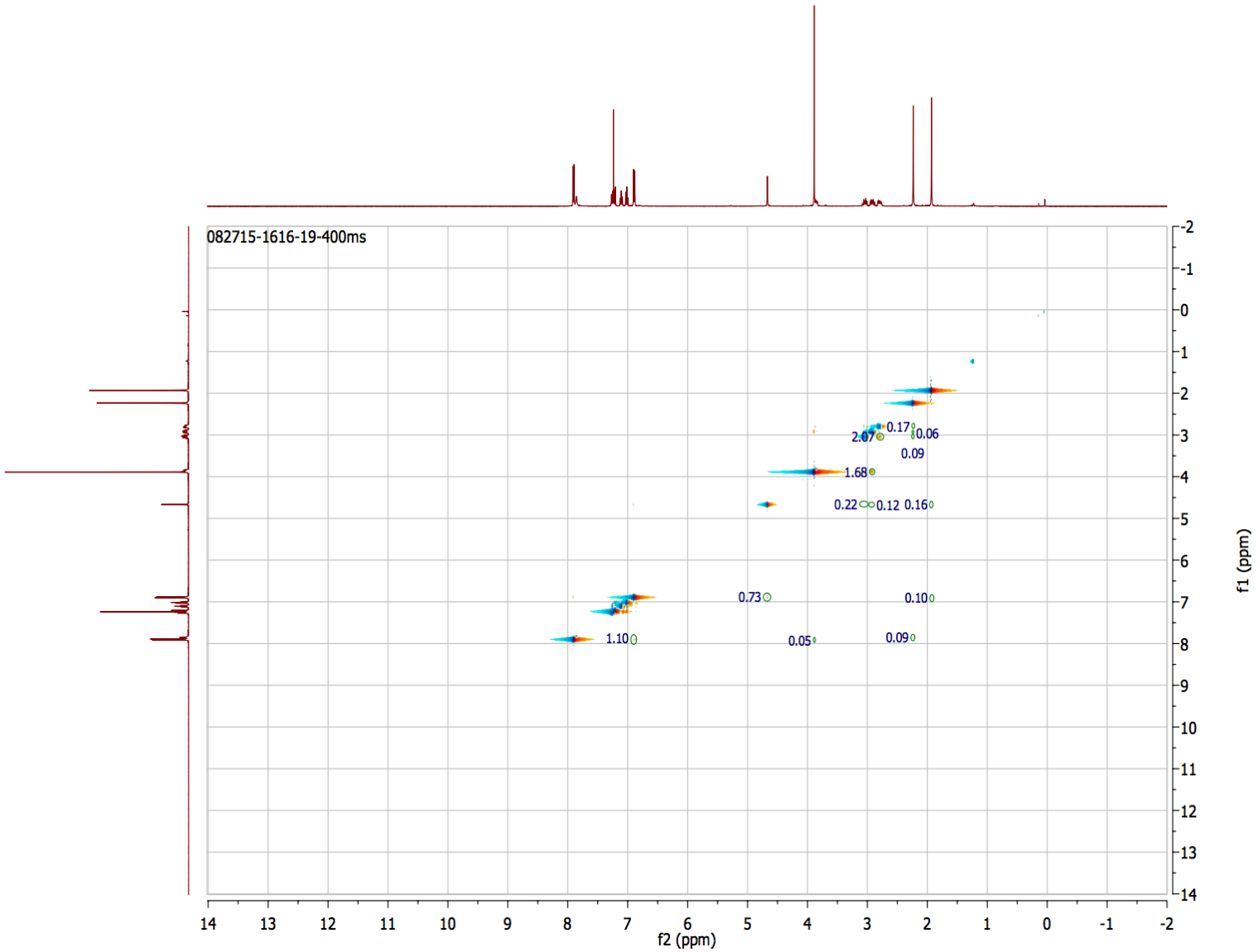

Figure S2: 2D NOESY NMR spectrum of PYD-106 (400ms)

A

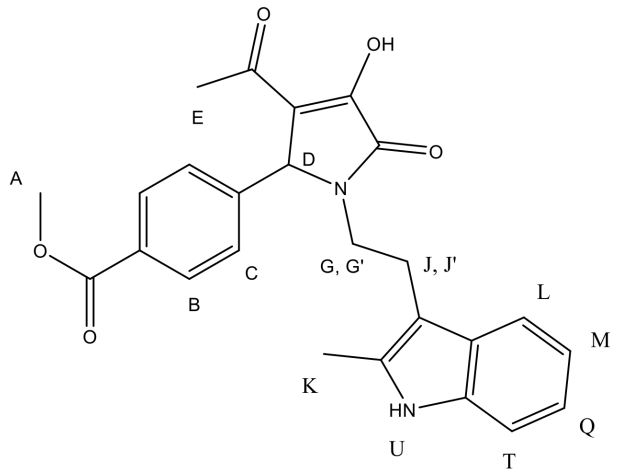

Proton Assignment Key

B

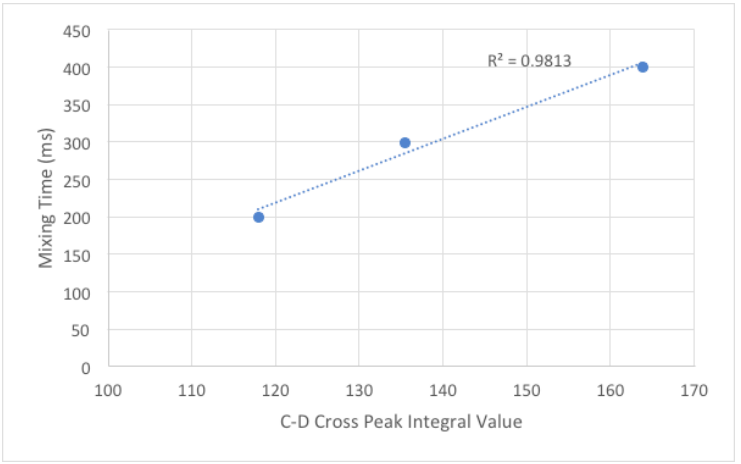

Linear Range Verification for C-D Cross Peak

C NMR Data Observed for Protons in PYD-106

Proton Identity	ppm	Multiplictiy (Coupling Constant, Hz)	Integration	Average NOESY Intensity
A	3.91	s	3	A to B (11.64)
B	7.93	d (8.0)	2	B to C (257.67)
C	6.92	d (8.4)	2	C to D (169.6); C to E (23.20)
D	4.69	s	1	
E	1.95	s	3	D to E (37.69)
G	3.90-3.86	m	1	D to G (28.71)
G'	2.98-2.90	d, t (13.6, 8)	1	G to G' (392.58)
J	3.10-3.03	d, t (13.6, 7.2)	1	D to J (51.00) J to J' (482.74)
J'	2.85-2.78	m	1	
K	2.26	s	3	K to J (19.86); K to G (14.27); K to J' (40.09)
L	7.24	7.8	1	
M	7.04	7.48	1	
Q	7.13	7.2	1	
T	7.28	8.04	1	
U	7.88	brs	1	K to U (21.61)

D Calculated Interatomic Distances for NOESY Partners

Nuclei	Interatomic Distance
A-B	4.16
B-C	2.48
C-D	2.66
C-E	3.70
D-E	3.42
D-G	3.58
G-G'	2.31
D-J	3.25
J-J'	2.23
K-J	3.80
K-G	4.02
K-J'	3.38
K-U	3.75

Figure S3: NMR experimental observations. (A) Proton Assignment Key, (B) Linear range verification for C-D cross peak, (C) NMR Data Observed for Protons in PYD-106, (D) Calculated interatomic distances for NOESY partners.

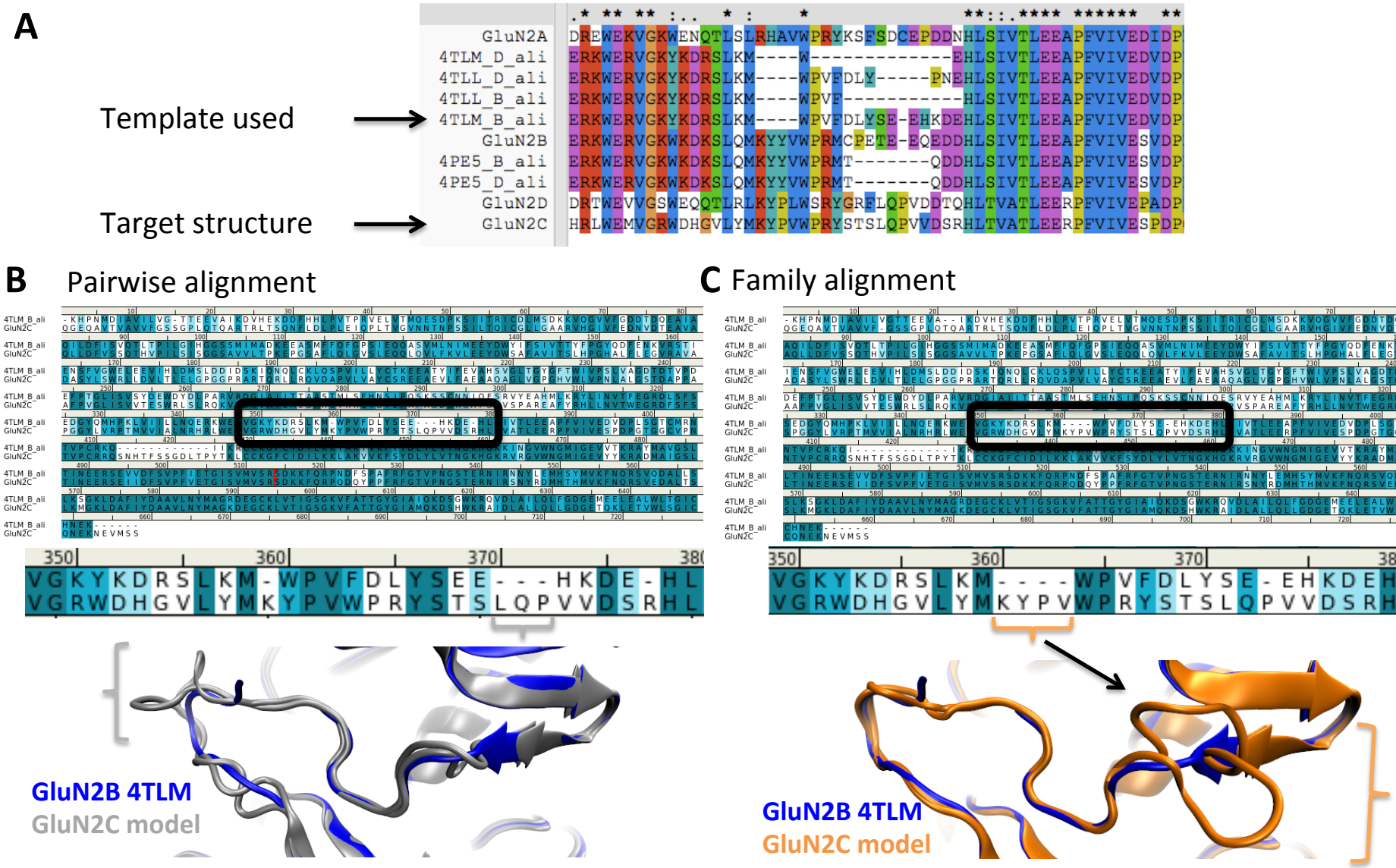

Figure S4: The alignment used for building in the linker region between ATD and ABD. (A) Multiple sequence alignment obtained from muscle. (B) The corrected alignment used in model building. (C) Incorrected family alignment. The homology model (orange) shows a bulge in the backbone indicated by arrow.

Supplemental Material S5: Attempt as separation of PYD enantiomers

In an effort to isolate the PYD enantiomers in sufficient amount for crystallization and x-ray crystallographic evaluation, several diastereospecific modifications were made to the PYD core structure using chiral reagents. These attempts include hydrolyzing the methyl benzoate ester and esterifying the resulting benzoic acid with (S)-(-)-phenylethanol and (R)-(+)-phenylethanol. Unfortunately both of the chiral esters produced inseparable diastereomeric mixtures. We also attempted separation of PYD enantiomers by using chiral amines ((R)-(+)-1-(1-naphthyl)ethylamine and (S)-(-)-1-(1-naphthyl)ethylamine) in the modified Biginelli cyclization reaction. The resulting products from these reactions again yielded products that could not be separated. Additionally, acylation of the enol OH of the PYD core with chiral phenyl glycine was attempted. This approach also resulted in an inseparable mixture of diastereomers.

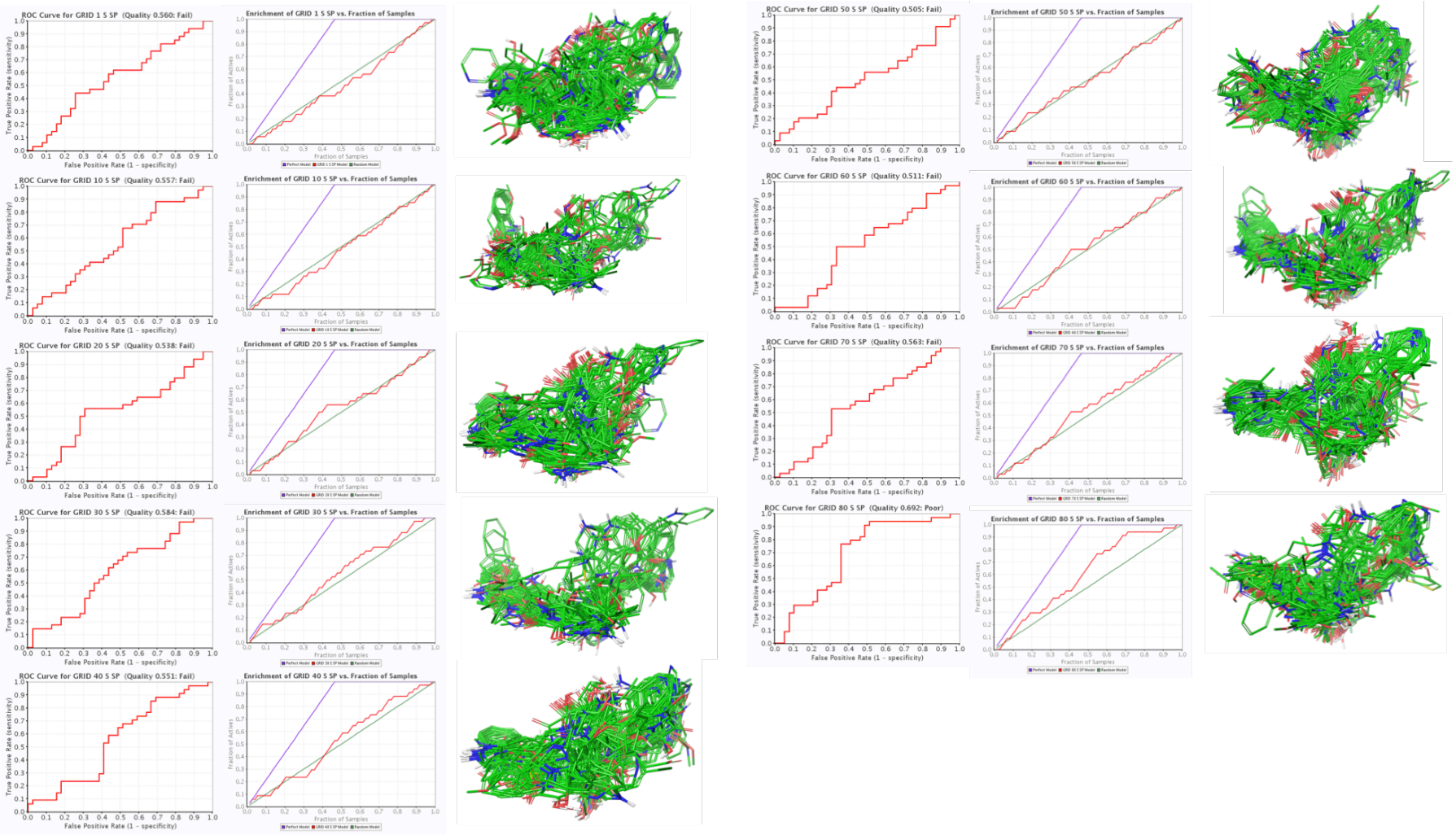

Figure S6: The ROC curves and Enrichment plots of the *S*-enantiomer of 79 compounds representative of the PYD series docked to 9 homology models. The 9 ROC plots and Enrichment plots are for homology model 1, 10, 20, 30, 40, 50, 60, 70 and 80. No clear pattern for the binding poses of the PYD series can be seen for any of the selected receptor structures.

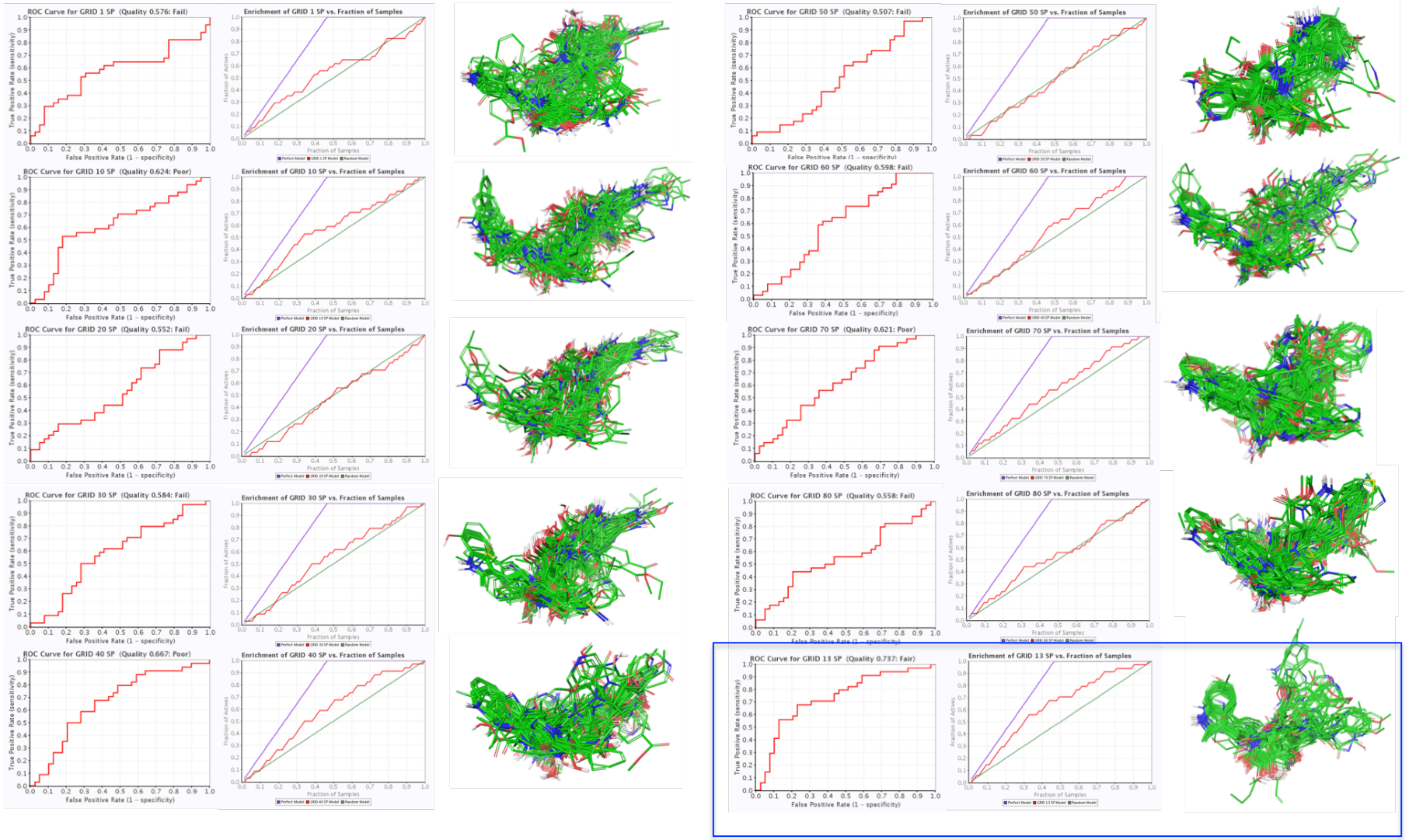

Figure S7: The ROC curves and Enrichment plots of the *R*-enantiomer of 79 compounds representative of the PYD series docked to 10 homology models. The first 9 ROC plots are for homology model 1, 10, 20, 30, 40, 50, 60, 70 and 80. The blue box highlights the ROC curve and enrichment plot for the selected homology model (13). A clear pattern for the binding poses of the PYD series can be seen in the selected receptor structure. The other receptor structure does not show a clear binding mode.

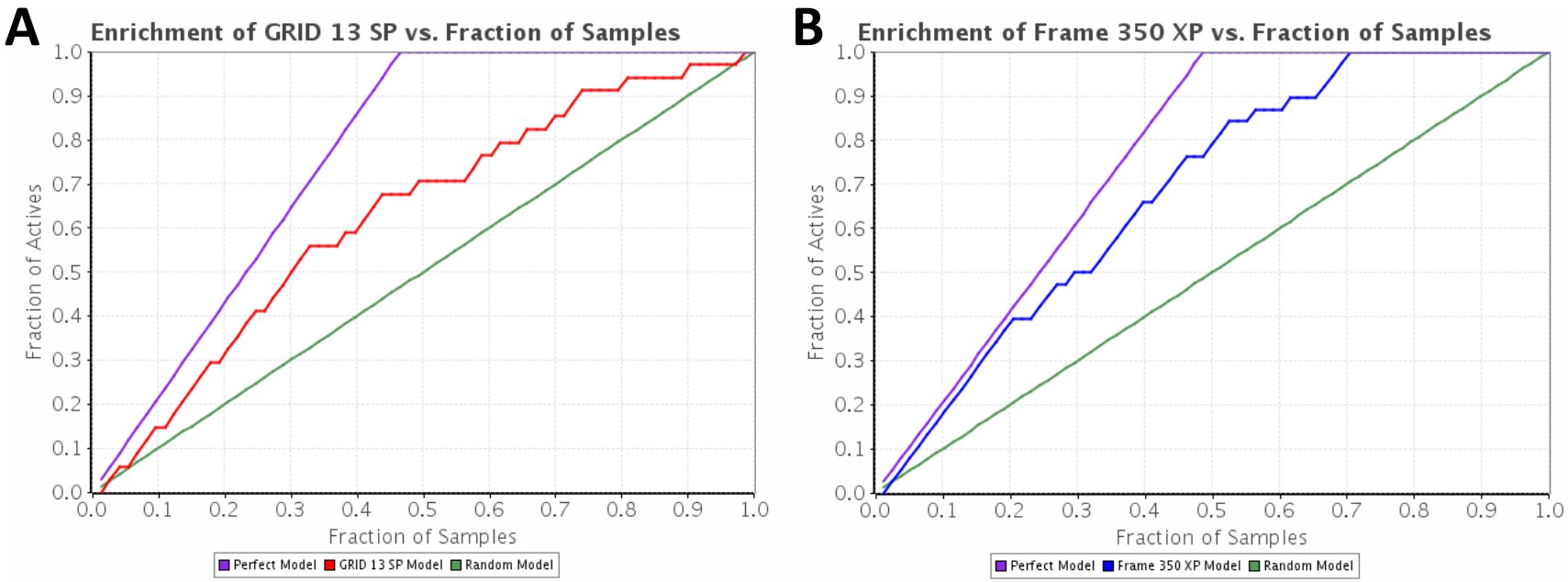

Figure S8: Enrichment plot for PYD-series docked against the selected GluN2C homology model (A) and a GluN2C structure (optimized using MD) after 3.5ns of simulation time (B).

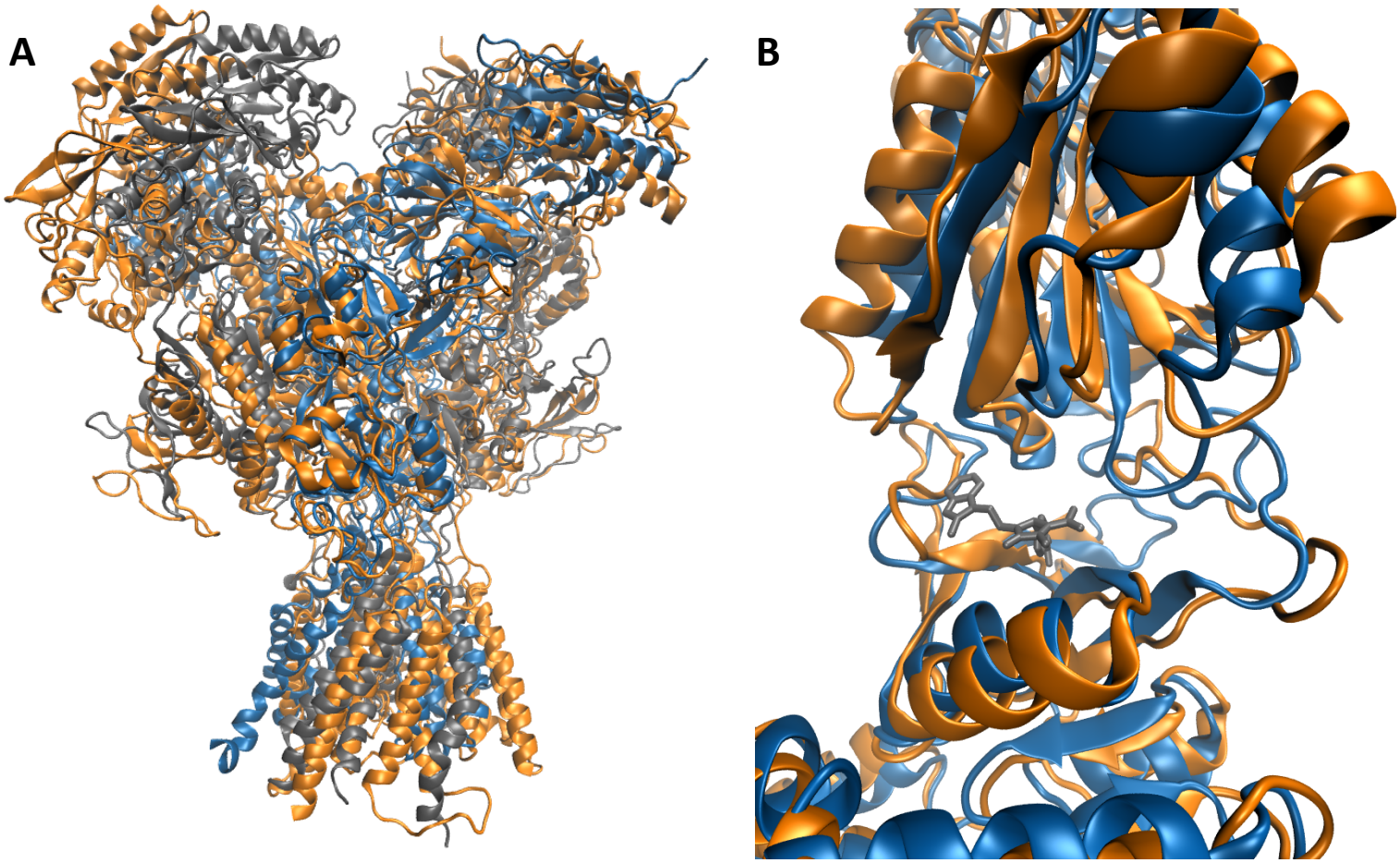

Figure S9: Molecular overlay of the GluN1/GluN2C diheteromeric homology model and a diheteromeric GluN1/GluN2B Cryo-EM structure (PDBID: 5IOU) **(A)** Full-length molecular overlay aligned based on GluN2C (Blue) and GluN2B (Orange) (B) The binding pockets of the GluN1/GluN2C PYD-106 diheteromeric complex (Blue) and of the GluN1/GluN2B diheteromeric Cryo-EM structure (Orange) bound with Gly and Glu are shown.

Table S1: Shared sequence identity and similarity between NMDA subunits of the PYD binding pocket

Identity/Similarity	GluN1	GluN2A	GluN2B	GluN2C	GluN2D
GluN1	**100/100**	23/49	23/49	23/46	23/46
GluN2A		**100/100**	71/94	60/74	60/86
GluN2B			**100/100**	66/80	63/89
GluN2C				**100/100**	57/80
GluN2D					**100/100**